Wind and Structures, *Vol. 23, No. 3 (2016) 191-209*
DOI: http://dx.doi.org/10.12989/was.2016.23.3.191

Wind tunnel study of wind structure at a mountainous bridge location

Lei Yan[1,2,4a], Zhen S. Guo[*1,3], Le D. Zhu[1,2,3b] and Richard G.J. Flay[4c]

[1]*Department of Bridge Engineering, Tongji University, 1239 Siping Road, Shanghai 200092, China*
[2]*State Key Laboratory of Disaster Reduction in Civil Engineering, Tongji University, 1239 Siping Road, Shanghai 200092, China*
[3]*Key Laboratory of Wind Resistance Technology of Bridges of Ministry of Transport, Tongji University, 1239 Siping Road, Shanghai 200092, China*
[4]*Department of Mechanical Engineering, The University of Auckland, Private Bag 92019, Auckland 1142, New Zealand*

(Received October 22, 2015, Revised June 15, 2016, Accepted June 18, 2016)

Abstract. Wind tunnel tests of a 1/2200-scale mountainous terrain model have been carried out to investigate local wind characteristics at a bridge location in southeast Tibet, China. Flows at five key locations on the bridge at deck level were measured for 26 directions. It was observed that wind characteristics (including mean wind velocity and overall turbulence intensity) vary significantly depending on the approaching wind direction and measurement position. The wind inclination angle measured in the study fluctuated between -18° and +16° and the ratio of mean wind velocity to reference wind velocity was small when the wind inclination angles were large, especially for positive wind inclination angles. The design standard wind speed and the minimum critical wind speed for flutter rely on the wind inclination angle and should be determined from the results of such tests. The variation of wind speed with wind inclination angles should be of the asymmetry step type. The turbulence characteristics of the wind were found to be similar to real atmospheric flows.

Keywords: mountainous terrain; approaching wind direction; wind inclination angle; turbulence characterization

1. Introduction

More and more cable-supported bridges within a mountainous area in southeast Tibet have been built to connect two districts. The subject of this study, namely Polonggou Bridge (95° E, 30° N), is located on the G318 Shanghai-Lhasa Expressway, in the Hengduan Mountains in southeast Tibet, China. It is a cable-stayed bridge with a mid-span of 430 m and a deck altitude of 2090 m. The bridge deck is 89 m above the riverbed which is basically without water all year round.

*Corresponding author, Senior Engineer, E-mail: guo@tongji.edu.cn
[a] Ph.D. Student, E-mail: yanlei0519@gmail.com
[b] Professor, E-mail: ledong@tongji.edu.cn
[c] Professor, E-mail: r.flay@auckland.ac.nz

http://www.techno-press.org/?journal=was&subpage=8 ISSN: 1226-6116 (Print), 1598-6225 (Online)

However, the observed river debris flow crest can rise to 2019 m in summer, or 71 m below the bridge deck on occasions. The surrounding terrain within a radius of 5 km comprises four large mountains with peaks rising to altitudes of approximately 4160 m, 3560 m, 3460 m and 4020 m. These are located to the north, east, south and west sides of the bridge respectively. There are four valleys between each pair of mountains. A schematic layout of Polonggou Bridge is shown in Fig. 1 and the location of bridge and its surrounding topography is shown in Fig. 2.

Mountains and valleys often act as physical barriers and channels to atmospheric flows and therefore significantly interrupt the normal global atmospheric circulation to create unique local wind conditions. The speed and direction of the wind can change dramatically and a far more turbulent wake region can form in the lee of mountains than over smooth terrain. Most research conducted in the last three decades has focused on wind speed-up effects, and little information has been provided on turbulence intensities, yaw angles and wind inclination angles in mountainous terrain.

Several empirical speed-up prediction algorithms have been published to provide formulae or look-up tables to predict speed-up for simple orography. EN 1991-1-4:2005 has adopted an orography factor that accounts for the increase of mean wind speed over isolated hills and escarpments (not undulating and mountainous regions). AS/NZS 1170.2:2011 also has a topographic multiplier for simple ideal topography, like hills, ridges and escarpments. JTG/T D60-01-2004 suggests that designers should undertake numerical simulations, field measurements or wind-tunnel simulations to predict wind speed-up and to determine design wind speeds for bridges proposed at sites with complex terrain.

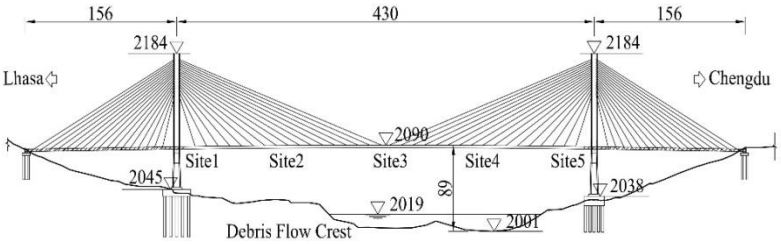

Fig. 1 Schematic layout of Polonggou Bridge (unit:m)

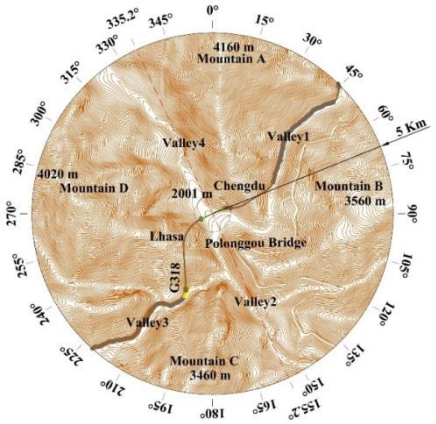

Fig. 2 The location of Polonggou Bridge within the surrounding topography

There has been great progress in the numerical evaluation of wind flows over different types of structure and topography (Blocken 2014). Ramechecandane and Gravdahl (2012) concluded that numerical simulations could generally perform well for the upstream but problematic predictions for the downstream regions of complex terrain.

Field measurement results of local wind characteristics for a specific site may not be available in situations of complex terrain. Cermak and Isyumov (1998) noted that in such situations small-scale topographic models, constructed at scales in the range of 1:1000 to 1:5000, can be effective for estimating the full-scale mean flow field. Bowen (1998, 2003) discussed some significant issues that affect the accuracy of wind-tunnel simulations of wind flows over complex terrain. Terrain model wind tunnel experiments were conducted for the Stonecutters Bridge site to study the wind turbulence characteristics (Hui *et al.* 2009a, b). The turbulence flow above the complex terrain along the Norwegian coastlines was investigated via wind tunnel test of terrain model for wind farms (Røkenes and Krogstad 2009). Wind tunnel tests described by Yeow *et al.* (2015) over Bolund Hill at two Reynolds numbers were carried out and their results compared with a satisfying degree of agreement with the full-scale results of Bolund blind comparison (Berg *et al*. 2011, Bechmann *et al.* 2011). Yang *et al.* (2015) observed the differences in the influences of wind characteristics on vortex-induced vibrations of a long-span suspension bridge between wind tunnel tests and full measurements

For flexible cable-supported bridges built in mountainous areas, the variability of the local wind characteristics with wind direction indicates that this poses a new and complicated challenge for wind-resistance bridge design and for research investigations. In the present study, a wind-tunnel simulation was carried out to investigate the wind characteristics at the proposed bridge site and to obtain wind parameters for the bridge, including design standard wind speeds at the bridge deck level and minimum critical wind speeds for flutter. Those results, and some turbulence structure data for the maximum wind speed at site 2 which occurred for the direction of 270° are presented and discussed in this paper.

2. Overview of the wind tunnel tests

2.1 Selection of model scale

In selecting the model scale, it is important to minimize the influence of the wind-tunnel walls and excessive blockage of the test section. Cermak and Isyumov (1998) noted that for a blockage ratio of 5% or less, distortion effects are negligible and a correction for the speed-up of the flow at the model is sufficient. Selection of the model scale should also consider measurement errors. There are three main sources of measurement error: the accuracy of the Cobra Probes, errors due to the position of the probe being slightly different from its correct measurement location, and errors due to incoming flow simulation.

Errors due to the incoming flow simulation is one of the three main sources of measurement errors in the study. The atmospheric turbulence of the mountainous region at inlet is very complex. On one hand, the zero plane displacement should be considered to obtain the effective height for the mean wind profile and it depends on the nature, height, and distribution of the roughness elements (Simu and Scanlan 1996); on the other hand, the mean wind profile usually cannot be described by the logarithmic law or the power law simply (Chen *et al.* 2008). Chen (2008) concluded that the wind characteristics of one site in such a complicated mountainous area mainly

depends on its surrounding barriers. It is generally hard to simulate the incoming wind characteristics in mountainous areas exactly in wind tunnel tests, and the simulation area of terrain should be large to reduce the influence of the atmospheric turbulence at inlet and the radius of selected simulation mountainous terrain is 5.0 km in this study.

The selected mountainous terrain area then extended radially from the center of the bridge deck for a distance of 6.05 km as a boundary transition section in order to avoid the abrupt change in terrain being too close to the test location (Hu *et al.* 2015). The terrain for the model only included the topography above an elevation of 2000 m, with the highest summit being 2160 m above this datum, with an average height of 1184.4 m, and the overall diameter of the terrain model was 12.1 km.

In order to remove the effects of blockage almost completely, the model scale would need to be 1: 5000, but then the measurements close to the ground at particular sites would have had significant inaccuracies due to the associated gross errors in modelling the local terrain. At this scale the deck upper surface at the mid-span and the tower top would have been at the low heights of 18.0 mm and 29.7 mm respectively above local ground level, and such low heights may have given rise to unacceptable measurement errors.

In a compromise between blockage effects and measurement accuracy, the terrain model was constructed at a geometric scale of 1 to 2200 using 10 mm thick high-density foam sheets. The average height of the terrain was 1184.4 m and the overall full-scale diameter was approximately 12.1 km corresponding to distances of 0.538 m and 5.5 m respectively on the model, giving an average wind tunnel blockage ratio of 9.9%. There were some local sections, especially summits where the effective height ratio was closer to 50% and flow stream-lines over the summit were expected to be definitely deflected by the roof. However, the region of most interest in the study was mainly at a height of 41 mm (corresponding to the bridge deck level) where the deflecting influence of the roof on the flow was expected to be small.

2.2 Wind tunnel equipment

The wind tunnel tests were carried out in the Tongji University (China), TJ-3 Wind Tunnel, which is a closed-circuit vertical return tunnel at Tongji University. Wind speed within the tunnel is continuously variable between 1.0 and 17.6 m/s and the working section is 14.0 m long, 15.0 m wide and 2.0 m high. A three-dimensional traversing system mounted to the ceiling allows for precise placement of a sensor at any point with an accuracy of 0.5 mm within the test section in the 1/2200-scale mountainous terrain model, corresponding to 1.1 m in the real atmosphere.

A Cobra Probe is a multi-hole pressure probe that provides dynamic, 3-component velocity, pressure and flow direction measurements in real time. Cobra Probes for the wind tunnel tests were available in various ranges for use between 2 m/s and 40 m/s and all could measure flow angles within a ±45° acceptance cone. The standard sign convention for the Cobra Probe was adopted, such that the yaw angle was positive when the approaching flow was deflected to come from the left looking upwind and vice versa. During the tests, the Cobra Probe was rotated to ensure that the mean wind vector was near the center of the cone of acceptance. Hence the measured yaw angle had to be corrected into the wind tunnel axes by adding the zero yaw angle (like the sunflower always turning towards the sun). The accuracy of one of the Cobra Probes was investigated and is shown in Table 1. It is clearly sufficiently accurate for this investigation.

Table 1 Cobra Probe accuracy for velocity and flow angle measurements

	Pitch-Yaw ±24°		Pitch-Yaw ±45°	
Test velocity (m/s)	Velocity Error (m/s)	Pitch-Yaw Error	Velocity Error (m/s)	Pitch-Yaw Error
3	±0.1	±1°	±0.3	±3°
12	±0.2	±0.3°	±0.3	±1°
40	±0.3	±0.2°	±0.6	±1°

During the wind tunnel tests, a Cobra Probe supported at the end of a steel arm attached to the internal traversing system was used to measure the wind characteristics at the desired locations. Another Cobra Probe was situated upstream of the terrain model at a height of 1000 mm and simultaneously measured the reference wind velocity. The reference wind velocity was approximately 10.5 m/s and the overall turbulence intensity was less than 2%. This low turbulence intensity occurred because the upwind wind tunnel fetch was smooth, thus simulating wind flow over a smooth flat surface. The oncoming flow had a very small boundary layer thickness and the lateral velocity uniformity was also good with less than ±1.9% variation. The Cobra Probe measurements were recorded at 1000 Hz for 65.5 s.

A photograph of the general layout of the model in the wind tunnel and the standard sign convention for the Cobra Probe is shown in Fig. 3 and a close up view of the model at the proposed bridge location is shown in Fig. 4.

2.3 Measurement sites

To obtain systematic wind characteristics at the bridge site, wind tunnel measurements at five key locations on the bridge deck were made for 24 directions at equi-spaced angles of 15°. Measurements were also made for two additional directions perpendicular to the longitudinal axis of the bridge. The terrain model was fixed on a wooden turntable on the wind tunnel floor, which allowed measurements at different wind directions by rotating the model. Details of the five measurement sites are shown in Fig. 5.

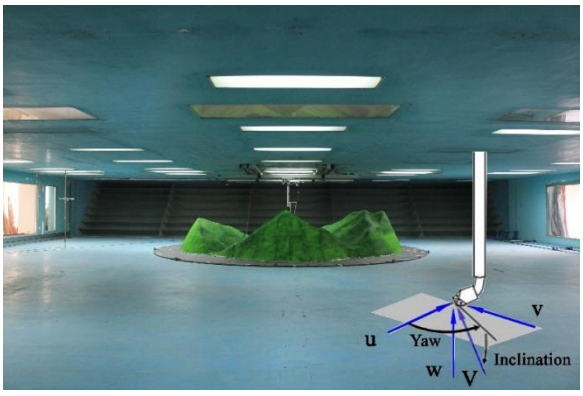

Fig. 3 The general layout of the model in the wind tunnel and the standard sign convention for the Cobra Probe. (The test section is 15 m wide and 2 m high and the model diameter is 5.5 m)

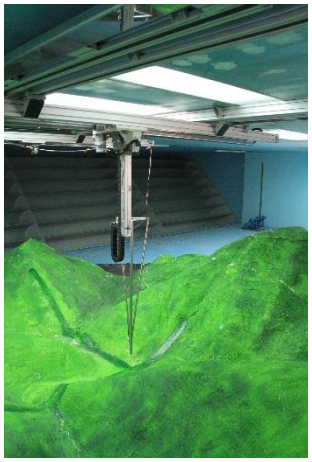

Fig. 4 A close up view of the model at the proposed bridge location

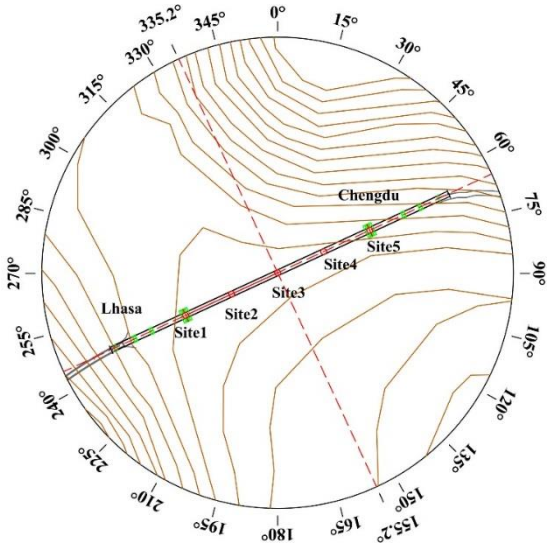

Fig. 5 Locations of the 5 measurement sites

3. Major test results

3.1 Variation of mean wind speed and overall turbulence intensity with approaching wind direction

Many different wind characteristics were measured from the five bridge sites at the bridge deck height of 41 mm for the 26 different approaching wind directions, but in this section only the mean

wind velocities and overall turbulence intensities are discussed. A summary of the mean velocity and turbulence intensity results is given in Figs. 6 and 7. The mean wind speed is presented in the form of U/U_{ref} , where U_{ref} is the reference wind speed measured upstream of the terrain model, as described in Section 2.2, and $I_{overall}$ stands for the overall turbulence intensity (i.e., it includes contributions from all the x, y and z directions). The mean wind speed ratios range between approximately 0.18 and 0.81 around the full circle due to the effects of the upwind terrain. The minimum value of U/U_{ref} is less than 0.18 at site 5 for a direction of 225° whist the maximum velocity ratio is 0.81 for Site 2 for the wind direction of 270° when the flow descends from an extremely high upwind summit. At such a low height, the obstacles in the path of the zigzag axis of valleys (e.g. the wind direction of 332.5°) may reduce the wind speed, and the wind velocity is also likely to be influenced by the boundary layers of the floor and the surrounding mountains. Conversely, the flow from the Mountain D probably descends steeply and encounters the front part of the Mountain A and then speeds up along the Valley 4. The latter flow movement path is supported by the fact that the yaw and inclination angles of wind speed at site 2 for a wind direction of 270° in the study are -65.7° with respect to the wind tunnel longitudinal direction (along Valley 4) and -5.1° (downwards). Similarly, the overall turbulence intensities vary dramatically from a low of about 16% for Site 1 for the wind direction of 300° to a high of approximately 52% at Site 5 when the direction is 30°. The majority of the turbulence intensity values are much larger than those recommended in EN 1991-1-4:2005, AS/NZS 1170.2:2011 or in JTG/T D60-01-2004 for such heights and terrain surface roughness. Furthermore, the overall turbulence intensity changes were found to vary inversely with the mean wind speed ratio. Both values change substantially with approaching wind direction as well as with measurement position on the bridge due to the effects of the very complex surrounding terrain.

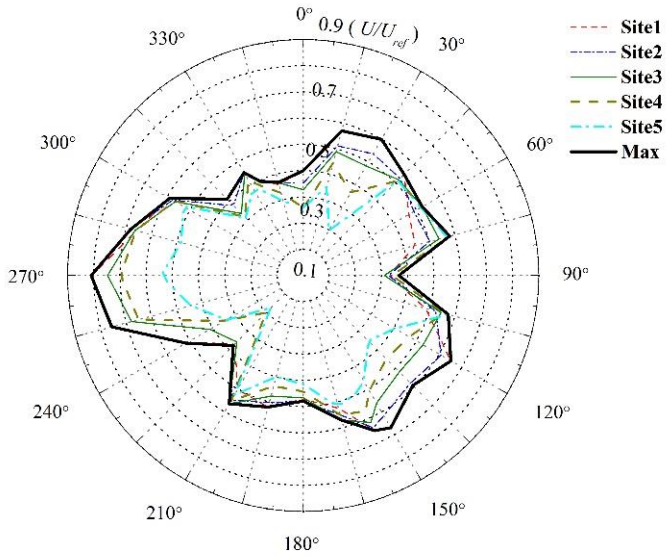

Fig. 6 Mean wind speed ratios as a function of approaching wind direction

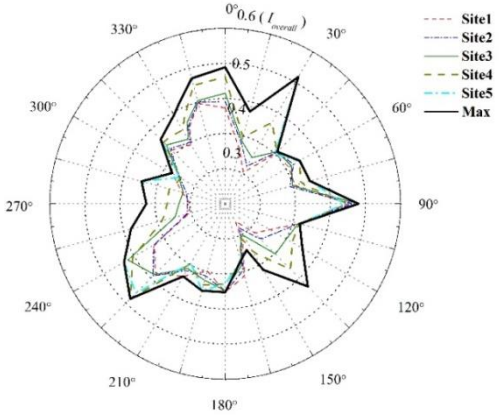

Fig. 7 Overall turbulence intensities as a function of approaching wind direction

3.2 Variation of wind inclination angle with approaching wind direction

The mean wind speed is the most important parameter for engineers to use to calculate wind loads on structures and for researchers to examine the wind-resistance performance of such structures. However, to investigate bridge aerodynamics, not only is it important to know the mean wind speed, but also the wind inclination angle is very important. A summary of the variation of the velocity ratio as a function of mean wind inclination angle is presented in Fig. 8. The wind inclination angles measured in this study varied between -18° and +16°. It is evident in Fig. 8 that the mean velocity ratios varied more widely for smaller inclination angles compared to the larger inclination angles. Furthermore, it can be seen from the curve enveloping the maximum values of velocity ratio that the maximum values of velocity ratio occur for small inclination angles and vice versa. The distributions of wind inclination angle at different points are different, and the distribution ranges of Site 4 and Site 5 are wider than those of Site 1, Site 2 and Site 3. It is shown in Fig. 5 that Site 4 and Site 5 are nearer to the Mountain A than Site 1, Site 2 and Site 3, so the wind speeds at Site 4 and Site 5 are likely to change more dramatically and the distributions of wind inclination angle at Site 1, Site 2 and Site 3 are similar due to the similar surrounding barriers.

3.3 Determination of the design standard wind speed and minimum critical wind speed for flutter

Without the availability of long-term field measurement wind velocity data at a bridge site, the gradient wind velocity V_G in the atmosphere can be calculated (in China) using the method given in JTG/T D60-01-2004. Using this method, the basic wind velocity at Nyingchi, southeast Tibet, namely, the characteristic 10-minute mean wind velocity at 10 m above ground level in the open country terrain (terrain category B) corresponding to a 100-year return period, is 29.7 m/s. In addition the exponent α of the mean wind power-law profile is about 0.16, and the height of the gradient wind is 350 m. Thus, the site gradient wind velocity V_G in the atmosphere for the serviceability limit state can be calculated in Eq. (1)

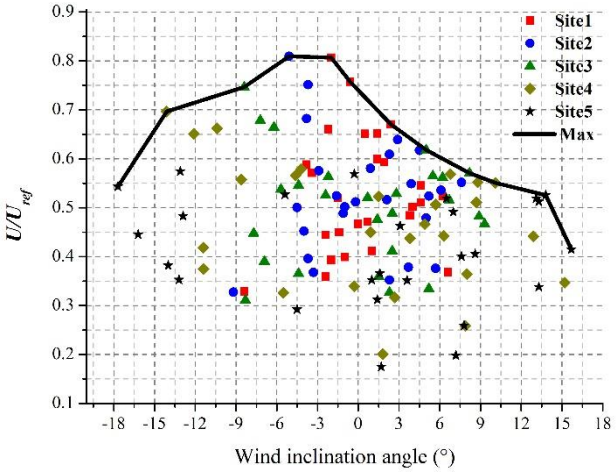

Fig. 8 Variation of velocity ratio as a function of wind inclination angle for all 5 measurement locations and all test wind directions

$$V_G = V_{10}(\frac{z_G}{z_{10}})^{\alpha} = 29.7 \times (\frac{350}{10})^{0.16} = 52.5\ (m/s). \tag{1}$$

As stated above, the reference wind velocity in the wind tunnel tests U_{ref}, was measured simultaneously with the wind velocity at the bridge and can be considered as V_G in the real atmosphere, and thus the design standard wind speed at different heights V_d can be calculated using the velocity ratio by Eq. (2)

$$V_d = \left(\frac{U_{model}}{U_{ref}}\right) \times V_G. \tag{2}$$

For the construction state, the appropriate return period is specified as 20 years in China, and the corresponding design reference wind speed V_d^s is determined using Eq. (3)

$$V_d^s = 0.88 \times V_d. \tag{3}$$

According to the Specification (JTG/T D60-01-2004), when examining flutter instability for bridges, wind tunnel tests should take into account the range of wind inclination angles between -3° and +3°. The specification is applicable to flat topography (coastal areas or flat plains), where large wind inclination angles are unlikely to occur for long return periods. For complex terrain, it is known that wind inclination angles may be larger than the above proposed range, which agrees with the present wind tunnel results. HSBA-1976 suggest that when the surrounding topography is complex, wind tunnel tests should take into account a range of wind inclination angles between -7° and +7°.

According to JTG/T D60-01-2004, the minimum critical wind speed for flutter is given by Eq. (4)

$$[V_{cr}] = K \times \mu_f \times V_{d0}, \tag{4}$$

where V_{d0} is the standard design wind speed at the deck level and μ_f is a synthetic coefficient which takes into account the influence of turbulence on wind speed and the incomplete correlation of winds along the bridge span. It depends on the local terrain conditions and the length of the bridge span, and is set to 1.394 for the present bridge. *K* is a safety factor which takes into account the uncertainties in wind tunnel tests for the design and construction of bridges, and is set to 1.2 in the present example.

The wind inclination angle at deck level measured in the wind tunnel in this study fluctuated dramatically between -18° and +16° as shown in Fig. 8. The values of the design standard wind speed at the deck level have been determined over 5 wind inclination angle intervals between -20° and +20°. In consideration of the possible measurement errors, the maximum value for safety at the five measurement sites for all 26 different wind directions has been chosen. If it is assumed that Eq. (4) is valid between -20° and +20°, then the minimum critical wind speeds for flutter can then be calculated and the wind tunnel test results can be used to determine the minimum critical flutter speed for the different wind inclination angles.

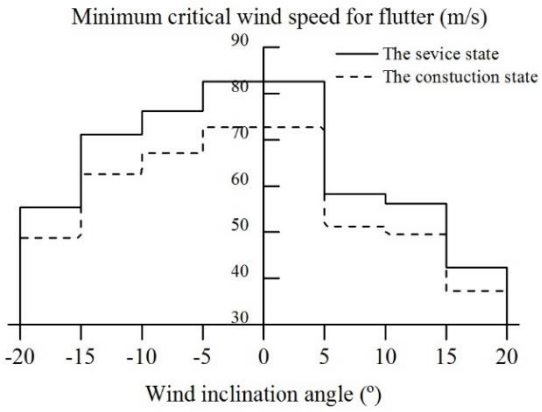

Fig. 9 Minimum critical wind speed for flutter as a function of wind inclination angle

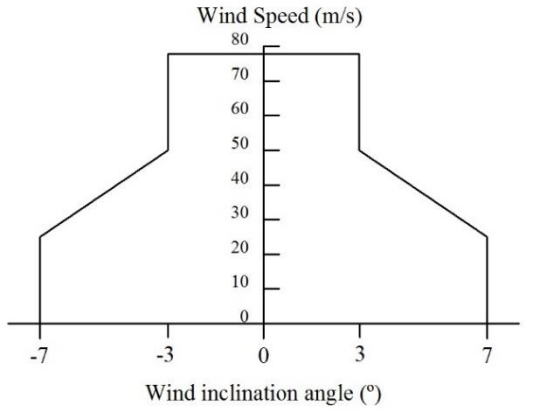

Fig. 10 Reference wind speed as a function of inclination angle

The calculated values of the minimum critical wind speed for flutter at different wind inclination angles are shown in Fig. 9 using the wind tunnel data. In the standard (HSBA-1976), the effect of velocity fluctuations is partly taken into account by considering the inclination of the mean wind, with the condition that there is no bias in real mean inclination angle at the construction site. A maximum inclination angle of 7° was determined as three times the average standard deviation of inclination angle with averaging time of 30 s (Fujino *et al.* 2012). The standard reference wind speed is shown in Fig. 10 as a function of inclination angle using the approach of Fujino *et al.* (2012).

It can be seen from the present wind tunnel results that wind inclination angles at bridge sites in mountainous terrain can be far larger than the suggested inclination angle of 7° in the standard for complex terrain. Fig. 8 shows that the maximum ratio of mean wind velocity to reference wind velocity is smaller when the wind inclination angle is large, especially for positive wind inclination angles, and vice versa. From the present results it is clear that the shape of the minimum critical wind speed for flutter as a function of wind inclination angle should be an asymmetry step-type in Fig. 9 and not be of the type shown in Fig. 10 in order to be conservative.

3.4 Comparison of the gradient wind velocity with Code/standard Provisions

There is a lack of long-term field measurement data of wind velocity at the bridge site, and so how to determine the gradient wind velocity with a 100-year return period in the real atmosphere (the reference wind velocity in wind tunnel tests) is of great importance. In this section, comparisons are made between different mean wind speed profiles recommended by different international codes and standards.

Most structural loading codes and standards (e.g., ASCE7-10, NBCC 2010, JTG/T D60-01-2004, AIJ-2004) use ‘‘power law’’ models of the planetary boundary layer velocity profile, developed in the 1960s, that assume the boundary layer rises to between about 250 and 500 m with a constant exponent, depending on exposure roughness (Kwon and Kareem 2013). Note that the power-law is not based on any theory, but is purely an empirical equation based on curve-fitting real data.

Another mean wind profile named the “logarithmic law” is adopted by micrometeorological researchers and a few design codes and standards e.g., (EN 1991-1-4:2005 for structures under 200 m). The logarithmic law is only valid in the constant shear stress layer which is about one-tenth of the depth of the atmospheric boundary layer (Tennekes 1973). For greater heights, the modified logarithmic law was recommended by Harris and Deaves (1981) and is used in the Australia/New Zealand wind loading standard (AS/NZS 1170.2:2011). It is based on more fundamental physical considerations and the gradient height is much higher, of the order of 2000 - 3000 m in strong winds and the gradient height z_G can be determined by Eq. (5)

$$z_G = \frac{1}{6}\frac{u*}{f_c}, \tag{5}$$

where $u*$ is the friction velocity, and f_c is the Coriolis parameter. In this study, $f_c = 7.27\times10^{-5}$ using the latitude of the Polonggou Bridge location which is 30° N.

The statistics of wind speed and direction used in wind engineering have traditionally been based on records over various periods of time recorded by ground-based meteorological stations, often with anemometers at heights of 10 m. The hourly wind speed is used by design purposes in NBCC2010 and Deaves and Harris model (which is used in AS/NZS 1170.2:2011). A 10-min wind speed is used in EN 1991-1-4:2005, JTG/T D60-01-2004 and AIJ-2004, whereas a 3-s gust speed

is used by ASCE7-10. The relationship between wind speeds averaged over different time intervals for winds above any type of surface should be considered for comparison purposes, and the following approximate relationship is given in Eq. (6) (Simiu 2011)

$$V_t(z) = V_{3600}(z)\left\{1 + \frac{\eta(z_0)c(t)}{2.5ln\frac{z}{z_0}}\right\}, \tag{6}$$

where $V_t(z)$ is the peak speed averaged overs t s with a record of approximately one hour, and $V_{3600}(z)$ is the hourly mean wind speed, over the terrain with surface roughness z_0 at the height of z. The function $\eta(z_0)$ (see Table 2(a)) is the ratio of the r.m.s of the longitudinal velocity fluctuations to the friction velocity. The coefficient $c(t)$ (see Table 2(b)) is an empirical peak factor which increases as t decreases.

As for NBCC2010 and Deaves and Harris model, the hourly wind speeds at 10 m above ground level in the open terrain were converted to 27.9 m/s and 28.1 m/s separately from the 10-min wind speed of 29.7 m/s by multiplying the ratios of 0.94 and 0.95 individually which are shown in Table 3. After calculating the corresponding hourly gradient wind velocities at the height of 274 m and 4137 m and then were converted to 10-min wind speeds divided by 0.96 and 0.97 one by one again. The peak 3-s gust speed in ASCE7-10 multiplied the ratio of 1.45 at the height of 10 m with 10-min wind speed of 29.7 m/s and then calculated the 3-s gradient wind velocity and divided it by the ratio of 1.32 at the gradient wind height of 274 m in the same way. The relationship between hourly wind speed or 3-s gust and 10-min wind speed above the open terrain is shown in Table 3.

Table 2a Factor $\eta(z_0)$ in Eq. (6)

z_0(m)	0.005	0.02	0.03	0.05	0.3	1
$\eta(z_0)$	2.55	2.47	2.45	2.44	2.30	2.20

Table 2b Factor $c(t)$ in Eq. (6)

t (s)	1	3	10	100	600	3600
c (t)	3.00	2.85	2.32	1.02	0.36	0.00

Table 3 The relationship between hourly mean wind speeds, and 3-s gust and 10-min wind speeds above open terrain

Code/Standard	t (s)	$c(t)$	$c(600)$	z_0 (m)	$\eta(z_0)$	$V_t(10)/V_{600}(10)$	z_G(m)	$V_t(z_G)/V_{600}(z)$
ASCE7-10	3	2.85	0.36	0.02*	2.47	1.45	274	1.32
NBCC2010	3600	0.00	0.36	0.05**	2.44	0.94	274	0.96
Deaves and Harris model	3600	0.00	0.36	0.02	2.47	0.95	4137	0.97

* Approximate value corresponding to ASCE7-10 Exposure C (ASCE Commentary Sect. C26.7)
** The value of roughness length z_0 in the open terrain is assumed to be 0.05 for comparison purposes

Table 4 10-min gradient wind velocities above the open terrain in different codes and standards

Code/Standard	α	z_0 (m)	u^*(m/s)	z_G (m)	V_G (m/s)
JTG/T D60-01-2004	0.16	0.05		350	52.5
AIJ-2004	0.15			350	50.6
ASCE7-10	0.11	0.02		274	47.4
NBCC2010	0.16			274	49.3
EN 1991-1-4:2005		0.05	2.24	z=350*	V_z=49.6
Deaves and Harris model		0.02	1.91	z=350**	V_z=47.9
Deaves and Harris model		0.02	1.91	4137	69.8

* The logarithmic law in EN 1991-1-4:2005 is assumed to be valid up to 350 m.
** Although the gradient wind height using the Harris and Deaves profile is much more than 350 m, the height and corresponding wind speed are used in this analysis for comparison purposes.

The gradient height in the open terrain is 350 m in JTG/T D60-01-2004 and AIJ-2004 and 274 m in ASCE7-10 and NBCC2010 and there is 76 m disparity (21.7%), but the 10-min gradient wind velocities are close to each other at approximately 50 m/s with only 9.7% difference between 52.5 m/s in JTG/T D60-01-2004 and 47.4 m/s in ASCE7-10. The gradient height obtained using the Deaves and Harris model (which was used to obtain the Height and Terrain Roughness Category Multipliers ($M_{z,cat}$) in AS/NZS 1170.2:2011) is 4137 m which is very high, much higher than other recommended values and results in a larger 10-min gradient wind speed of 69.8 m/s. For comparison purposes, the maximum applied height in EN 1991-1-4:2005 using the logarithmic law is assumed to be 350 m and that height is also added in AS/NZS 1170.2:2011 and those two 10-min wind speeds at that height are close to 50 m/s again. The 10-min gradient wind velocities above open terrain using the approaches from the different codes and standards are shown in Table 4.

3.5 Turbulence characterization of approaching wind flow for a direction of 270°

For the Polonggou Bridge site, the outcomes above indicate that the maximum mean wind speed occurs at Site 2 for a wind direction of 270°. According to Fig. 2, the flow descends onto the bridge from an extremely high summit upwind for that direction. It appears that this extreme upwind terrain causes the observed high wind speed phenomenon.

3.5.1 Mean flow characterization

The 65.5-second-averaged mean wind speed, and the azimuth and inclination of the mean wind are analyzed using a MATLAB computer program. The mean wind speed is 9.3 m/s and the yaw and inclination angles are -65.7° with respect to the wind tunnel longitudinal direction (along Valley 4) and -5.1° (downwards). It can be seen from Table 1 that the velocity and the pitch-yaw errors of the Cobra probe are less than 0.2 and 0.3 respectively, so are reasonably insignificant.

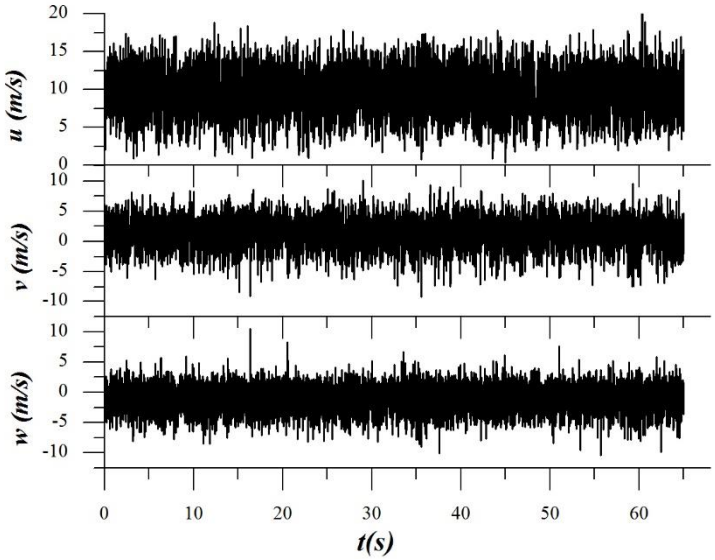

Fig. 11 Time histories of the *u*, *v* and *w* velocity components at Site 2, for a wind direction of 270°

3.5.2 Turbulence intensities and Integral scales of turbulence

The 65.5-second time histories of the velocity components for Site 2 are shown in Fig. 11 and the measured values and ratios of the components of turbulence intensity are calculated and given in Table 5. It can be seen that the measured values of turbulence intensity are larger than those specified in JTG/T D60-01-2004 for terrain category D, or in EN 1991-1-4:2005 and AS/NZS 1170.2:2011 for the longitudinal component, and the ratios are close to accepted values published by Flay (1978), Fu *et al.* (2008) and Hui *et al.* (2009a).

Table 5 Measured and specified values, and ratios of turbulence intensity

Values				Ratios		
	I_u (%)	I_v (%)	I_w (%)		I_v/I_u	I_w/I_u
Measurement	27.2	20.3	16.4	Measurement	0.74	0.60
Terrain D in the specification JTG/T D60-01-2004	22.0	19.4	11.0	Flay (1978)	0.79	0.49
Terrain IV in the code EN 1991-1-4:2005	22.2	-	-	Fu *et al.* (2008)	0.80	0.70
Terrain category 4 in the code AS/NZS 1170.2:2011	24.0	-	-	Hui *et al.* (2009a)	0.85	0.60

The integral scales of turbulence are measurements of the average size of the turbulent eddies of the flow. The three integral length scales in the longitudinal direction, L_u^x , L_v^x and L_w^x are often estimated from the corresponding integral time scales based on Taylor's hypothesis of convected "frozen turbulence" (Batchelor 1953), namely, it is assumed that the flow disturbance travels at the mean wind speed U without any decay (Simiu and Scanlan 1996). Therefore the calculation of integral length scale can be obtained from the corresponding integral time scale as shown in Eq. (7).

$$L_a^r = \int_0^\infty Cov_a(r)dr/\sigma_a^2 = U\int_0^\infty c_a(\tau)d\tau, \tag{7}$$

where $a = u, v, w$ and U is the mean wind speed along the longitudinal direction; $Cov_a(r)$ is the auto-covariance function of turbulence component of a and $c_a(r)$ is the corresponding normalized auto-covariance function which is equal to unity at zero time-lag. The exponential decay law (Eq. (8)) can also be fitted to such data up to the first zero crossing and used to find the parameter λ, which is the inverse of the integral time scale in Eq. (8).

$$\mathrm{c_a}(\tau) = \exp(-\lambda\tau) \tag{8}$$

The integral length scale of the turbulence component "a" in direction "r" is given by Eq. (9).

$$L_a^r = U/\lambda \tag{9}$$

Normalized auto-covariance curves of the three velocity components deduced from the measured data are fitted to exponential decay curves to determine as λ shown in Fig. 12. The corresponding values of the integral scales of turbulence in the longitudinal direction are given in Table 6. It can be seen that exponential decay curves fit the measured auto-covariance data well, and the value of L_w^x is close to the value recommended by Teunissen (1992). The integral scales are relate to the size of the surrounding barriers and the volumes of mountains and valleys in the terrain model are very large in this terrain model, so the integral scale in such a complex terrain are larger than it in the plains.

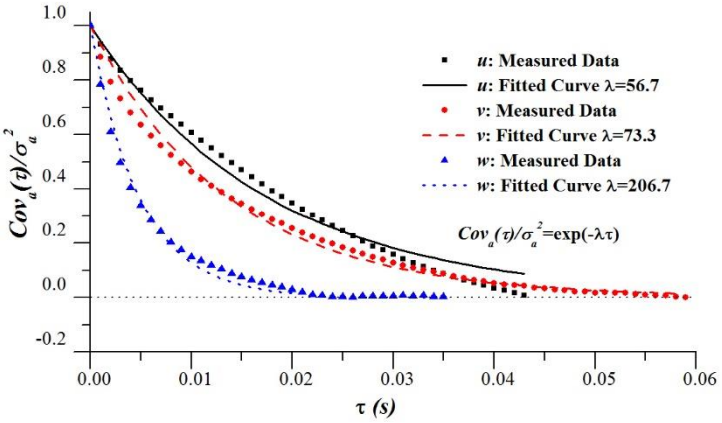

Fig. 12 Normalized auto-covariances of the *u*, *v* and *w* velocity components

Table 6 Values of integral length scales in the longitudinal direction

	L_u^x (m)	L_v^x (m)	L_w^x (m)
Measurement	0.164	0.127	0.045
Corresponding to full scale	358.6	279.4	99
JTG/T D60-01-2004	140	70	
Teunissen (1992)	104		71.2

3.5.3 Velocity spectra

The non-dimensional power-spectral density represents the distribution of the kinetic energy of the wind eddies in the frequency domain. According to the literature (e.g., Zhu 2002), all three non-dimensional power-spectral densities can be fitted by the expression given in Eq. (10)

$$\frac{fS_a}{{\sigma_a}^2} = \frac{af_L}{(1+bf_L^{1/m})^{5m/3}}, \tag{10}$$

where the reduced frequency is given by Eq. (11).

$$f_L = fL_a^x/U \tag{11}$$

a, *b* and *m* are parameters needed to fit the curve to measured data and σ_a is the standard deviation of the velocity fluctuations of *a*. L_a^x are the length scales in the longitudinal direction of the velocity fluctuations of *a*, calculated as described in Section 3.5.2.

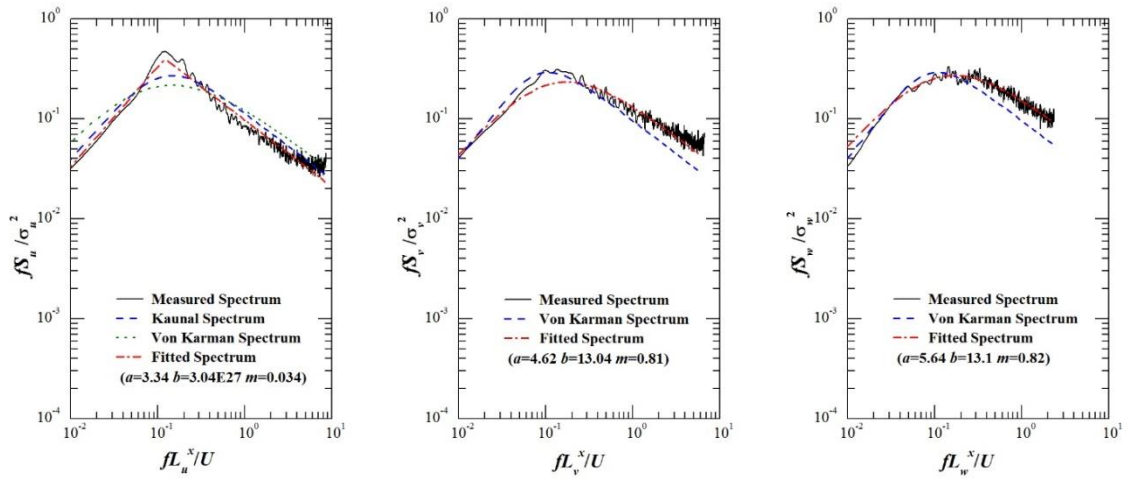

Fig. 13 Power-spectral density of the *u*, *v* and *w* velocity components

Non-dimensional power-spectral densities of the three turbulence components are shown in Fig. 13. It can be seen that the recommended expression (Eq. (10)) fits measurement data well both in the low-frequency region and at higher frequencies. The expressions recommended by Von Karman (1948) fit the measured data reasonably well for the longitudinal direction and the other directions in the low-frequency regions. However, the spectral equations given by Kaimal *et al.* (1972) for the longitudinal velocity component do not fit the data as well as the other expressions.

4. Conclusions

- The mean wind velocities and overall turbulence intensities vary significantly as a function of wind direction and the site measurement position on the model bridge deck.
- The local topography has a significant effect on the turbulence intensity, especially when the approaching flow descends from a summit, and the maximum overall turbulence intensity profile (along the approaching wind direction) basically follows the opposite trend of the corresponding mean wind, which is at least partially due to the mean speed being in the denominator of the turbulence intensity definition.
- The wind inclination angle measured in this study varied between -18° and +16°, and the ratios of the mean wind velocities at the bridge deck to the reference wind velocity were small when the wind inclination angles were large, especially for positive (flow upwards) wind inclination angles.
- The design standard wind speed and the minimum critical wind speed for bridge deck flutter rely on the wind inclination angle and these should be determined over a wide range of inclination angles when bridges are located in complex terrain. It is recommended that the shape of wind speed variation as a function of wind inclination angle should be of the "asymmetry step type".
- Comparisons of the gradient wind velocity among different codes and standards were made and the majority of provisions give a 10-min gradient wind velocity of approximately 50 m/s, whereas the Deaves and Harris approach, which was used to set up the tables of $M_{z,cat}$ in AS/NZS 1170.2:2011, gave a much larger gradient height and a correspondingly larger gradient wind speed.
- It was shown that the turbulence characterization of the approaching wind flow for a direction of 270° is similar to the real atmosphere on the basis of estimates of the turbulence intensity, the power spectral density, and the x-direction integral length scales.

Acknowledgements

The work described in this paper was supported by the National Natural Science Foundation of China (Grant 91215302) and China Scholarship Council. The opinions and concluding remarks presented in this paper are entirely those of the writers.

References

American Society of Civil Engineers (2010), *ASCE7-10 Minimum design loads for buildings and other structures*, ASCE, Reston, Virginia.

Architectural Institute of Japan (2004), *AIJ-2004 Recommendations for Loads on Buildings*, AIJ, Tokyo.

Batchelor, G.K. (1953), *The theory of homogeneous turbulence*, Cambridge University Press.

Bechmann, A., Sørensen, N.N., Berg, J., Mann, J. and Réthoré, P.E. (2011), "The Bolund Experiment, Part II: Blind comparison of microscale flow models", *Bound. – Lay. Meteorol.*, **141**(2), 245-271.

Berg, J., Mann, J., Bechmann, A., Courtney, M. and Jørgensen, H.E. (2011), "The bolund experiment, Part I: Flow over a steep, three-dimensional hill", *Bound. – Lay. Meteorol.*, **141**(2), 219-243.

Blocken, B. (2014), "50 years of computational wind engineering: Past, present and future", *J. Wind Eng. Ind. Aerod.*, **129**, 69-102.

Bowen, A.J. (1998), "Some complications from modelling the wind flow over complex terrain at small geometric scales", *Proceedings of the 13th Australasian Fluid Mechanics Conference*, Monash University, Melbourne, Australia, December.

Bowen, A.J. (2003), "Modelling of strong wind flows over complex terrain at small geometric scales", *J. Wind Eng. Ind. Aerod.*, **91**(12-15), 1859-1871.

Cermak, J.E. and Isyumov, N. (1998), *Wind tunnel studies of buildings and structures*, American Society of Civil Engineers, Virginia.

Chen, Z.Q. (2008), Terrain model test of wind field characteristics of the Aizhai Bridge (in Chinese), Wind Engineering Research Center, Hunan University, Changsha, China.

Chen, Z.Q., Li, C.G., Zhang, Z.T. and Liao, J.H. (2008), "Model test study of wind field characteristics of long-span bridge site in mountainous valley terrain (in Chinese)", *J. Exper. Fluid Mech.*, **22**(3), 54-59+67.

European Committee for Standardization (2005), *EN 1991-1-4:2005 Eurocode 1: Actions on structures-Part 1-4: General actions-Wind actions*, CEN, Brussels.

Flay, R.G.J. (1978), "Structure of a rural atmospheric boundary layer near the ground", Ph.D. Dissertation, University of Canterbury, Canterbury.

Fu, J.Y., Li, Q.S., Wu, J.R., Xiao, Y.Q. and Song, L.L. (2008), "Field measurements of boundary layer wind characteristics and wind-induced responses of super-tall buildings", *J. Wind Eng. Ind. Aerod.*, **96**(8-9), 1332-1358.

Fujino, Y., Kimura, K. and Tanaka, H. (2012), *Wind Resistant Design of Bridges in Japan*, Springer.

Harris, R.I. and Deaves, D.M. (1981), "The structure of strong winds", Wind Engineering in the Eighties Proceedings of the CIRIA conference held on 12/13 November 1980, London, UK.

Honshu-Shikoku Bridge Authority (1976), *HSBA-1976 Wind Resistant Design Standard (in Japanese)*, HSBA, Kobe.

Hu, P., Li, Y.L., Huang, G.Q., Kang, R. and Liao, H.L. (2015), "The appropriate shape of the boundary transition section for a mountain-gorge terrain model in a wind tunnel test", *Wind Struct.*, **20**(1), 15-36.

Hui, M.C.H., Larsen, A. and Xiang, H.F. (2009), "Wind turbulence characteristics study at the Stonecutters Bridge site: Part I—Mean wind and turbulence intensities", *J. Wind Eng. Ind. Aerod.*, **97**(1), 22-36.

Hui, M.C.H., Larsen, A. and Xiang, H.F. (2009), "Wind turbulence characteristics study at the Stonecutters Bridge site: Part II: Wind power spectra, integral length scales and coherences", *J. Wind Eng. Ind. Aerod.*, **97**(1), 48-59.

Kaimal, J.C, Wyngaard, J.C., Izumi, Y. and Cote, O.R. (1972), "Spectral characteristics of surface-layer turbulence", *Q. J. Roy. Meteorol. Soc.*, **98**(417), 563-589.

Kwon, D.K. and Kareem, A. (2013), "Comparative study of major international wind codes and standards for wind effects on tall buildings", *Eng. Struct.*, **51**, 23-35.

Ministry of Communication of PRC (2004), *JTG/T D60-01-2004 Wind-resistant Design Specification for Highway Bridges (in Chinese)*, China Communications Press, Beijing.

National Research Council of Canada (2010), *National Building Code User's Guide-Structural Commentaries (Part 4), Canadian Commission on Building and Fire Codes*, NRCC, Ottawa.

Ramechecandane, S. and Gravdahl, A. (2012), "Numerical investigations on wind flow over complex terrain", *Wind Eng.*, **36**(3), 273-296.
Røkenes, K. and Krogstad, P.Å. (2009), "Wind tunnel simulation of terrain effects on wind farm siting", *Wind Energy*, **12**(4), 391-410.
Simiu, E. (2011), *Design of buildings for wind a guide for ASCE 7-10 standard users and designers of special structures*, (2nd Ed.), John Wiley & Sons, Inc.
Simiu, E. and Scanlan, R.H. (1996), *Wind effects on structures: fundamentals and applications to design*, (3rd Ed.), John Wiley & Sons, Inc.
Standards Australia/Standards New Zealand (2011), *AS/NZS 1170.2:2011 Structural design actions Part 2: Wind actions*, Sydney and Wellington.
Tennekes, H. (1973), "The logarithmic wind profile", *J. Atmos. Sci.*, **30**(2), 234-238.
Tieleman, H.W. (1992), "Wind characteristics in the surface layer over heterogeneous terrain", *J. Wind Eng. Ind. Aerod.*, **41**(1), 329-340.
Von Karman, T. (1948), "Progress in the statistical theory of turbulence", *Proceedings of the National Academy of Sciences of the United States of America*, **34**(11), 530.
Yang, Y.X., Ma, T.T. and Ge, Y.J. (2015), "Evaluation on bridge dynamic properties and VIV performance based on wind tunnel test and field measurement", *Wind Struct.*, **20**(6), 719-737.
Yeow, T.S., Cuerva-Tejero, A. and Perez-Alvarez, J. (2015), "Reproducing the Bolund experiment in wind tunnel", *Wind Energy*, **18**(1), 153-169.
Zhu, L.D. (2002), "Buffeting response of long span cable-supported bridges under skew winds: field measurement and analysis", Ph.D. Dissertation, The Hong Kong Polytechnic University, Hong Kong.

CC